

Decay history and magnetic moments at high spin in ^{152}Dy

M. Hass*

Nuclear Structure Research Laboratory, University of Rochester, Rochester, New York 14627

N. Benczer-Koller and G. Kumbartzki

Rutgers University, New Brunswick, New Jersey 08903

T. Lauritsen, T. L. Khoo, I. Ahmad, M. P. Carpenter, R. V. F. Janssens, E. F. Moore, and
F. L. H. Wolfs[†]

Argonne National Laboratory, Argonne, Illinois 60439

Ph. Benet

Purdue University, West Lafayette, Indiana 47907

K. Beard

University of Notre Dame, Notre Dame, Indiana 47907

(Received 24 June 1991)

Average magnetic moments as well as information on the time evolution of the continuum structure of ^{152}Dy at high spin have been obtained using the transient hyperfine magnetic field acting on fast ions traversing a thin, magnetized gadolinium foil. ^{152}Dy nuclei were populated by the $^{76}\text{Ge}(^{80}\text{Se},4n)^{152}\text{Dy}$ fusion-evaporation reaction at $E(^{80}\text{Se})=326.5$ MeV. The target-ferromagnet arrangement corresponds to a time window of about $70 < t < 1100$ fs, during which the excited nuclei experience the transient field interaction. The statistical γ rays, as well as the high-energy, $E_\gamma > 1200$ keV, γ rays contributing to the collective $E2$ "bump," exhibit a negligible precession, in accordance with the very short lifetimes of these states. The precession of the angular distribution of discrete yrast γ rays deexciting the nucleus from spin $I \sim 35\hbar$ down yields an average magnetic moment for states with $43\hbar \geq I \geq 31\hbar$. The resulting $\langle g \rangle = 0.21(2)$ is considerably lower than the collective value $Z/A \sim 0.43$ and indicates an appreciable contribution from aligned neutrons to the lower-spin region populated within the above time frame. The results are discussed in the framework of model calculations of the γ -ray cascade.

I. INTRODUCTION

The measurements of g factors of high-spin nuclear states have received a new impetus from the improved theoretical understanding of shell effects in deformed potentials as well as from the availability of modern, high sensitivity, multidetector arrays. The experimental determination of magnetic moments has traditionally played an important role in the evolution of nuclear structure models since these moments probe mostly the single-particle degrees of freedom, in contrast to $E2$ properties which probe collective features. As an example, the measurements of g factors of high-spin levels in ^{158}Dy and in ^{238}U and ^{232}Th using the transient field technique have unambiguously determined the role of neutron and proton alignments in the structure of the backbending region [1,2]. Previously, only a few spin precession experiments have been carried out for the higher-spin regime. The most notable were experiments [3] on $^{153-156}\text{Dy}$, where average g factors for $20\hbar < I < 30\hbar$ were determined, and the experiments [4,5] on $^{158,160,162}\text{Yb}$, where yet higher-spin states were probed.

The evolution of nuclear properties with changes in angular momentum I and internal excitation energy above the yrast line U has been the subject of many investiga-

tions. So far, most studies examine γ -ray spectra, multiplicities and the appropriate Doppler shifts in order to determine decay schemes and to understand how nuclear structure changes in the spin-excitation energy plane. In particular, ^{152}Dy is a nucleus for which the evolution of the nuclear structure with increasing spin and internal energy has been exhaustively studied by a plethora of experiments which measured spectra, lifetimes, and angular distributions of continuum and discrete transitions [6]. It has been determined that the yrast states consist of oblate aligned-particle configurations. However, the excited states above the yrast line show evidence of collectivity, clearly reflected by a prominent quasicontinuum $E2$ "bump" [6].

In view of the available knowledge of the ^{152}Dy structure and of the intense theoretical interest generated more recently by the discovery of the superdeformed shape in this nucleus, the present study was undertaken with the two distinct goals of determining, from a spin precession measurement, both the time evolution of the nuclear decay and the magnetic moment of the states involved.

The time evolution of the nuclear decay can be followed after population of the highest-energy states through the complex decay pattern of statistical γ rays,

the continuum $E2$ “bump,” the dipole radiations and the weak discrete states that immediately precede the yrast line. As in all other experiments on short-lived nuclear states, the transient field technique [7] was used. This technique makes use of a large hyperfine interaction experienced by fast nuclei traversing ferromagnetic foils. This procedure provides a time window of about 70–1100 fs during which the ^{152}Dy ions traverse the magnetized gadolinium foil. The decay history can then be traced by following the magnetic precession of the relevant states sequentially populated as the nucleus decays.

The present experiment, coupled to existing models for the γ -ray flow from the entry point in the I - U plane down to the yrast line, provides information concerning the time evolution of the nuclear decay as well as the relative contribution of neutrons and protons to the total spin for the ensemble of nuclear states which is probed within the time window.

II. EXPERIMENT

High-spin levels in ^{152}Dy were populated with the $^{76}\text{Ge}(^{80}\text{Se},4n)^{152}\text{Dy}$ reaction using a 326.5-MeV beam from the ATLAS Facility. This particular reaction was selected to provide high recoil velocity to the ^{152}Dy nuclei. The high velocity insures that recoiling ions do not stop in the gadolinium foil (see discussion in Ref. [7]). The target layer of 1 mg/cm² of enriched ^{76}Ge was directly deposited on 6.6 mg/cm² of gadolinium, evaporated onto a 1 mg/cm² tantalum foil and backed by a 15 mg/cm² gold foil which provides a perturbation-free environment for the recoils to stop in. The target assembly was held between two permanent magnets in a setup similar to that used in a previous g factor measurement on ^{147}Gd [8]. The target was cooled by flowing liquid nitrogen to 100 K and the magnetization of the gadolinium foil was measured at this temperature (see Ref. [8]). The details of the target structure as well as the kinematics used in the reaction are presented in Table I. The target assembly is shown schematically in Fig. 1, together with the corresponding time scale for the ^{152}Dy nuclei traversing the target and ferromagnet [9]. As discussed below, the transit time through the ferromagnetic foil provides the relevant parameter needed to extract both the time history and magnetic moment information from the present results.

The present experimental setup made use of the

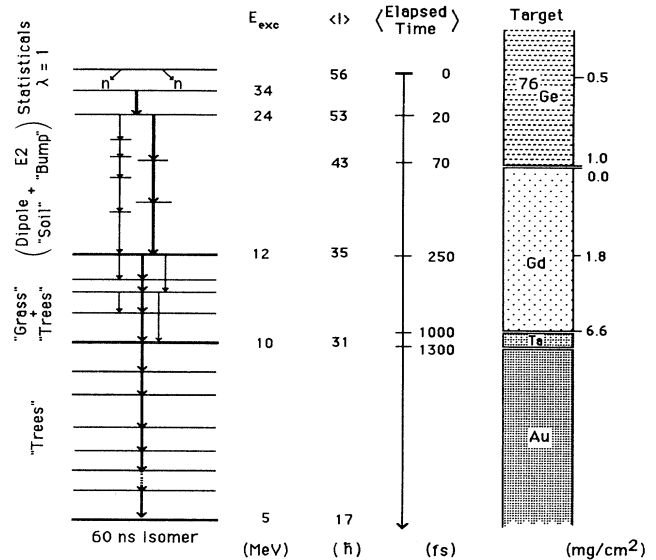


FIG. 1. Schematic view of the target assembly; the time scale for the recoiling ^{152}Dy nuclei is derived from the kinematics, with the average $t=0$ being taken in the middle of the ^{76}Ge layer. Also depicted are the average spin, excitation energy, and a schematic decay pattern as derived from the Monte Carlo simulations described in the text.

Argonne–Notre Dame BGO γ -ray facility. This apparatus consists of two rings of six Compton-suppressed detectors each, placed at 17° above and below the horizontal plane. Eight detectors located in the horizontal plane, at angles of $\pm 35.5^\circ$ and $\pm 144.5^\circ$ with respect to the beam direction, were used to determine the precession effect while the four remaining detectors at 90° served as checks for geometrical and systematic effects. Channel selection of ^{152}Dy was performed by tagging on the 60-ns isomer detected with an inner array of 46 hexagonal BGO detectors.

A typical spectrum of prompt γ rays measured in a backward detector, gated by a delayed multiplicity $3 < M < 8$, is shown in Fig. 2. The strongest features of the spectrum are the statistical γ rays at high energy, the collective $E2$ structure peaking at $E_\gamma \sim 1250$ keV, and the discrete transitions. Figure 3 presents a partial level scheme emphasizing the transitions whose precessions were measured in this experiment [10,11].

TABLE I. Description of the target composition and kinematics of the reaction. l represents the thickness of the target isotope while L is the thickness of the gadolinium foil. M is the magnetization of the ferromagnetic layer in an external field of $H_{\text{ext}}=0.14\text{T}$. $(v/v_0)_{\text{in}}$ and $(v/v_0)_{\text{out}}$ are the average ^{152}Dy velocities at the entrance and exit of the gadolinium foil in units of the Bohr velocity $v_0=e^2/\hbar$.

$l(^{76}\text{Ge})$	$L(^{\text{nat}}\text{Gd})$	M	$E(^{80}\text{Se})$	$E_{\text{in}}(^{152}\text{Dy})$	$E_{\text{out}}(^{152}\text{Dy})$	$\left[\frac{v}{v_0}\right]_{\text{in}}$	$\left[\frac{v}{v_0}\right]_{\text{out}}$
(mg/cm ²)	(mg/cm ²)	(T)	(MeV)	(MeV)	(MeV)		
1.0	6.6	0.2045	326.5	138.4	20.5	6.1	2.3

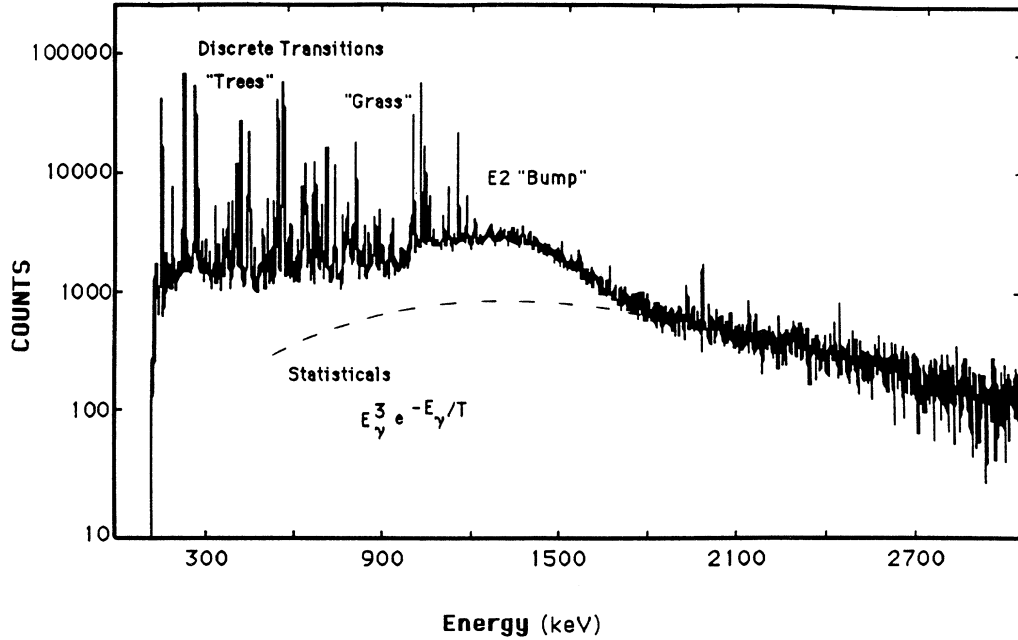


FIG. 2. A typical γ spectrum in a backward detector with the delayed multiplicity condition of $3 < M < 8$. The statistical γ rays, the $E2$ continuum, and the discrete transitions are easily discerned. The dashed line corresponds to a fit of the statistical radiations from 2000 to 3000 keV to the function $N(E_\gamma) = E_\gamma^3 \exp(-E_\gamma/T)$.

III. ANALYSIS

The analysis of the precession of the statistical γ rays, the $E2$ continuum, and the discrete transitions was carried out on “unfolded” spectra. These were obtained by a procedure designed to correct for the detector response and described in a previous publication [12]. A fit to the statistical radiations, corresponding to a spectral shape given by $N(E_\gamma) = E_\gamma^3 \exp(-E_\gamma/T)$, was subtracted from the data. The analysis of the precession of the statistical and discrete radiations was also carried out on the raw data, yielding essentially the same results.

Standard double ratios were formed as described in Ref. [7]:

$$\rho_{ij} = \left[\frac{N\uparrow(i)/N\downarrow(i)}{N\uparrow(j)/N\downarrow(j)} \right]^{1/2}, \quad (1)$$

where $N\uparrow(i,j)$ and $N\downarrow(i,j)$ represents, for example, the integrated counts in a given energy bin with magnetic field “up” or “down” for detectors i or j ($i, j = 1, 4$ or $2, 3$), located at the complementary angles of $\pm 35.5^\circ$ ($1, 4$) and $\pm 144.5^\circ$ ($2, 3$).

Ratios $\rho = (\rho_{14}/\rho_{23})^{1/2}$ were then obtained from which the precession effect, $\epsilon = (\rho - 1)/(\rho + 1)$, was calculated. Similar “cross ratios” $\rho_c = (\rho_{24}/\rho_{13})$ and ϵ_c were also evaluated in order to check for systematic effects that might mask the true precession [7]. In all cases, vanishingly small ρ_c were obtained, as expected. In addition,

the transitions below the 21^- , $\tau_{1/2} = 10.0$ ns, isomer exhibit no precession. This occurrence is expected because the time scale for paramagnetic relaxation of dysprosium in gold is much shorter than the mean life of the isomer.

In order to extract from the data of Table II either g factors of the high-spin states or the time evolution of the decay, further experimental input is still required. First, the angular distribution of the relevant γ rays has to be known. The ratios of counts at 35.5° and 144.5° to the counts at 90° were compared to the previous measurement of angular distributions [6], and were found to be in agreement. Hence, the angular distribution coefficients from the earlier experiment were adopted in the analysis carried out here, both for the discrete transitions and for the continuum spectra. The logarithmic slope S of the angular distribution $W(\theta)$ at the angle at which the measurements were carried out, $S = (1/W)(dW/d\theta)$, was obtained from these coefficients and the angular precession $\Delta\theta = \epsilon/S$ was calculated. The resulting values for S and $\Delta\theta$ for the discrete lines, and for the continuum radiation grouped in energy bins of 100 keV, are shown in Table II.

Second, the velocity dependence of the transient field has to be known to relate accumulated precession to elapsed time and to extract absolute values for the average magnetic moments. The Chalk River parametrization [13]

$$B(v, Z) = 154.7Z(v/v_0) \exp(-0.135v/v_0)M, \quad (2)$$

where $v_0 = e^2/\hbar$ is the Bohr velocity, was used for the

analysis. The calibration constant determined in Ref. [13] has been rewritten in terms of the foil magnetization M . The Ziegler stopping powers were utilized [14]. A typical uncertainty in this parametrization is of the order of 10% [7]. Figure 4 presents the precession results together with the corresponding energy regions of the γ -ray spectrum.

Finally, the g factor can be obtained from the relation

$$\Delta\theta = -(g\mu_N/\hbar) \int B(v(t), Z) dt, \quad (3)$$

where the integration is carried over the time the ^{152}Dy ion spends in the gadolinium foil.

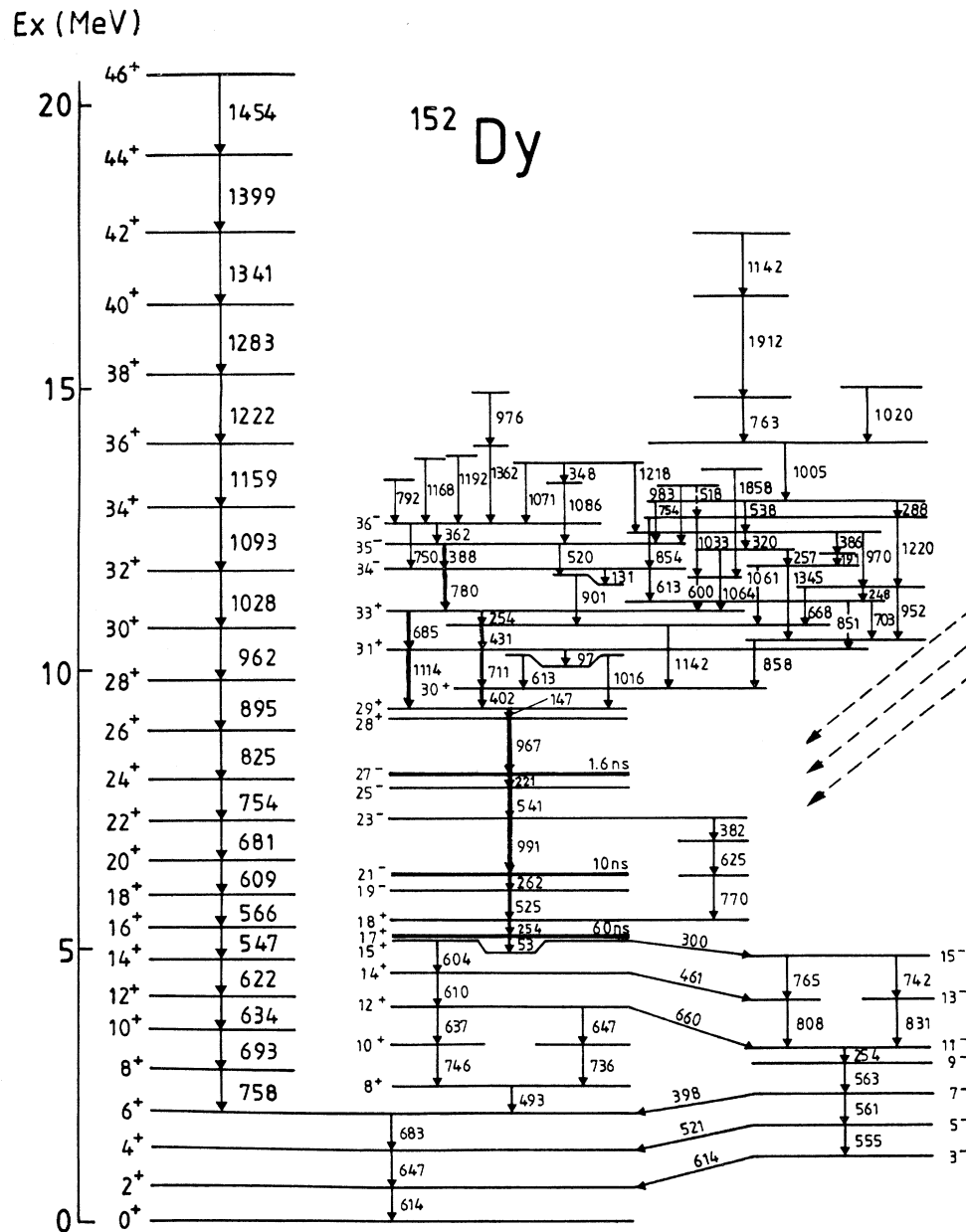


FIG. 3. Level scheme of ^{152}Dy (Refs. [10,11]). The bold lines indicate the transitions whose precessions were measured in this experiment. The dashed lines suggest the decay out of the superdeformed band not shown in this figure.

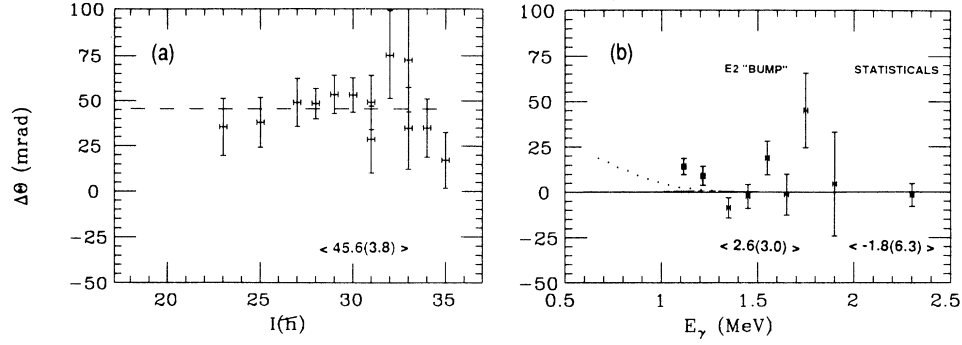


FIG. 4. Precession angles of the (a) discrete transitions vs I . The dashed line represents the average of the measured precessions; (b) statistical and $E2$ transitions vs E_γ . The dotted line is the result of the Monte Carlo calculation described in the text. The values indicated within brackets are the average $\Delta\theta$ for the region.

IV. RESULTS AND DISCUSSION

The data were interpreted according to the following model for the decay patterns. The paths followed by the decaying ^{152}Dy nuclei can be approximately classified into three different, overlapping categories. At first, after neutron evaporation, the hot nuclei decay very quickly by

statistical radiations intermingled with fast, high-energy, $E2$ transitions. The time scale for the early statistical radiations has been estimated in Ref. [1] to be of the order of 20 fs. Hence, most of the high-energy statistical γ rays are emitted before the nucleus even leaves the target and no precession effect ought to be noticed.

The second region covers the multitude of $E2$ transi-

TABLE II. Summary of precession angles $\Delta\theta$ for the statistical, $E2$, and discrete radiations. S represents the logarithmic slope of the angular correlations at angles of $\pm 35.5^\circ$ and $\pm 144.5^\circ$.

Energy (keV)	M^π	I^π	τ	S^a	$\Delta\theta$ (mrad)
Continuum					
> 2200	$\lambda = 1$			-0.39	-1.8(6.3)
1800-2000	$E2$			+0.41	+4.5(28.5)
1700-1800					+45.0(20.5)
1600-1700					-1.3(11.3)
1500-1600					+18.8(9.3)
1400-1500					-2.3(6.6)
1300-1400					-8.6(5.6)
1200-1300					+8.5(5.2)
					$\langle \Delta\theta \rangle = 2.6(3.0)$
1100-1200					+13.4(4.4)
Discrete transitions					
388	$M1$	35^-		-0.539	17.2(15.4)
780	$M1$	34^-		-0.480	35.0(16.0)
685	$E2$	33^+		+0.316	34.8(22.5)
254 ^b	$M1$	33^+		-0.500	72.4(28.6)
431	$M1$	32^+		-0.230	75.2(23.9)
1114	$E2$	31^+		+0.392	28.6(18.4)
711	$M1$	31^+		-0.685	49.1(15.0)
402	$M1$	30^+		-0.500	53.2(9.6)
147	$M1$	29^+	50 ps	-0.539	53.4(10.6)
967	$M1$	28^+		-0.500	48.4(8.4)
221	$E2$	27^-	2 ns	+0.210	49.0(13.3)
541	$E2$	25^-		+0.210	38.1(13.8)
991	$E2$	23^-		+0.234	35.5(15.8)
					$\langle \Delta\theta \rangle = 45.6(3.8)$

^a1986 measurement of the slopes (private communication).

^bThe 254-keV line is a doublet. The intensity ratio of the 254-keV $33^+ \rightarrow 32^+$ to the 254-keV $18^- \rightarrow 17^+$ transitions is taken from Ref. [10]. Assuming $S=0$ for the lower transition and $S=-0.5$ for the upper transition, the quoted $\Delta\theta$ is obtained.

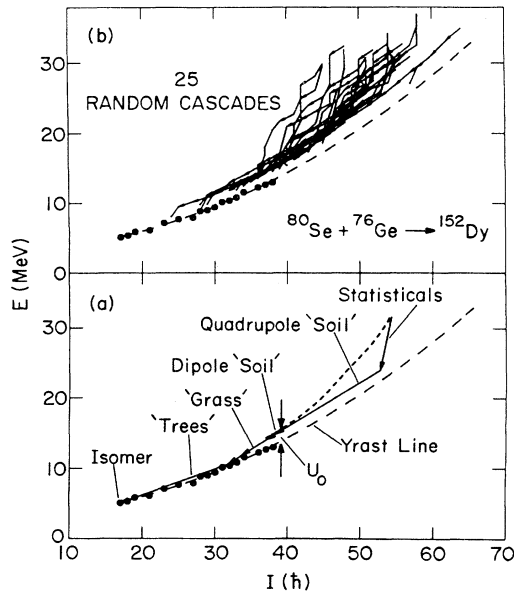


FIG. 5. Monte Carlo simulations: (a) Schematic representation of the average paths for different components of the γ spectrum for the $^{76}\text{Ge}(^{80}\text{Se},4n)^{152}\text{Dy}$ reaction. (b) Sample of simulated cascades generated using $\langle Q \rangle_t = 7 \text{ eb}$ and $\langle J \rangle = 76\hbar^2 / \text{MeV}$ (Ref. [6]).

tions contributing to the $E2$ “bump.” The lifetime experiments of Ref. [6] suggest that these processes last of the order of a few hundred fs. The analysis of the present data could, in principle, directly test this evaluation. However, due to the fact that the discrete transitions overlap in energy with the lower-energy γ rays of the $E2$ “bump,” only the high-energy part of the region can be directly measured.

Subsequently, the decay path approaches the vicinity of the yrast line via discrete, long-lived ($\sim 1 \text{ ps}$) (“grass”) states [6]. Finally, long after the nucleus leaves the gadolinium foil, it emerges into the yrast structure characterized by the well resolved γ -ray lines (“trees”). The observed precession of these transitions reflects the integrated precession of both the nuclear states which give rise to the low-energy part of the $E2$ “bump,” and the following dipole transitions. A schematic representation of the decay paths as determined in previous work is displayed in Fig. 5.

A. Continuum transitions

Several observations can be made immediately from the data displayed in Table II. The statistical γ rays indeed show no precession. This result is consistent with the expectation of the very short-lived nature of the very high-spin states. Although not strictly a lifetime measurement, this result constitutes a direct confirmation of the very fast decay of the statistical transitions.

The precession observed for the continuum $E2$ radiations in the energy range $1200 < E_\gamma < 2000 \text{ keV}$, $\langle \Delta\theta \rangle = 2.65(3.0) \text{ mrad}$, is vanishingly small, suggesting

that the corresponding states either have no magnetic moment, a rather unlikely occurrence for collective states which are expected to have a g factor of the order of $g \sim Z/A$, or are so short lived that they decay before the nuclei enter the ferromagnetic foil. A mean upper limit $t(E2, E_\gamma > 1200 \text{ keV}) \sim 70 \text{ fs}$ for the decay of the corresponding ^{152}Dy nuclei is obtained from the mean transit time through the ^{76}Ge target.

For the very narrow range $1100 < E_\gamma < 1200 \text{ keV}$, a finite precession is evident, $\Delta\theta = 13.4(4.4) \text{ mrad}$, indicating that the ^{152}Dy nuclei in this region of the $E2$ continuum are finally in transit through the gadolinium foil. The energy range of the $E2$ “bump” below 1100 keV cannot be analyzed for precession because the spectrum is dominated by the discrete transitions.

B. Discrete transitions: Probe states

The integral precession of the lower states in the $E2$ “bump” does, however, contribute to the precession displayed by the probe states deexciting via the discrete transitions. These lines, emitted long after the recoiling nuclei have left the ferromagnet, exhibit a much larger precession. The average of the values of $\Delta\theta$ for the discrete lines (Table II) yields $\langle \Delta\theta \rangle = 45.6(3.8) \text{ mrad}$. This precession corresponds to the “total” cumulative precession of the lower-energy $E2$ states together with “soil” and “grass” levels incurred by the ^{152}Dy nuclei while traversing the gadolinium foil, and yields an average g factor for the ensemble of states $\langle g \rangle = 0.21(2)$. This result is significantly lower than the value of Z/A expected for collective rotations, and suggests that aligned neutron configurations make appreciable contributions.

C. Monte Carlo simulation

In order to extract from this result either g factors or, alternatively, the time evolution of the decay, a model must be invoked. A Monte Carlo approach had been used to calculate the spectra of the quasicontinuum γ rays [6]. The model was very successful in simultaneously reproducing the spectral shapes, multiplicities, and yrast feeding region, and yielded an average transition quadrupole moment for the $E2$ transitions, $\langle Q \rangle_t = 7 \text{ eb}$, and average effective moment of inertia of $\langle J \rangle_{\text{eff}} = 76\hbar^2 / \text{MeV}$. The model has now been extended to calculate the spin rotation accompanying the passage of the fusion residues through the polarized ferromagnetic foil.

The starting point in the model is the measured mean entry point which represents the mean spin and excitation energy after the last particle is evaporated [15]. The entry distribution is chosen with widths in spin and excitation energy around this measured mean entry point. The γ -ray cascade starts from this entry distribution and involves competing statistical $E1$ and collective $E2$ emissions. The $E1$ decay is determined by the level density parameter [16] and uses a standard γ -ray strength function [17]. The $E2$ decay is characterized by a moment of inertia J , which determines the transition energy scale,

and a quadrupole moment $\langle Q \rangle_t$, which affects the overall transition rate. Rotational damping [18,19] is also taken into account.

The continuum cascades are terminated when the excitation energy over the yrast line lies below an experimentally measured [6] threshold energy $\langle U \rangle_0 \sim 1.5$ MeV, namely, where the cascade enters the “grass” region (Fig. 5). The decreased level density at this point begins to give rise to discrete transitions which feed into the yrast line over a time interval of a few ps. Using the model, the average spin precession angle can be associated with the γ -ray emission energy and compared to the observed rotation angle. The connection between decay times and transit through the gadolinium foil is schematically illustrated in Fig. 1, which shows that the total precession occurs in the gadolinium in the time interval of ~ 70 to 1100 fs. The calculation indicates that, on average, emission of the statistical, collective $E2$, and dipole radiations brings the nucleus down from spin $\langle I \rangle \sim 56\hbar$ to $\langle I \rangle \sim 35\hbar$ over a time period of approximately 250 fs. The remainder of the time is spent in “grass” and “tree” transitions of spin $31\hbar < I < 35\hbar$.

D. Semiempirical modeling

A simplified picture of these complex decays can help to elucidate the qualitative aspects of the present results. A two zone model may be invoked, in which one assumes that the nuclear states that contribute to the collective $E2$ “bump” have a g factor $g = Z/A = 0.43$; furthermore, the Monte Carlo modeling of the decay together with the experimental evidence from Ref. [6] indicate that, on average, the nuclei in the $E2$ “bump” spend about 180 fs in the gadolinium foil. The precession of the “dipole soil” and “grass” states through the rest of the foil can hence be calculated, and yields a g factor $\langle g \rangle = 0.14(2)$. This small value of the moment implies considerable contributions from aligned neutrons at spins $31\hbar < I < 35\hbar$.

To extract separate contributions to the precession and hence a precise picture of the evolution of the decaying structure, additional experiments are being prepared with a thinner gadolinium foil (~ 2 mg/cm²) which would only probe the medium-energy $E2$ structure. Conversely, a second experiment with a buffer layer between the ⁷⁶Ge target and the gadolinium, corresponding to a time delay of approximately 250 fs, will yield an independent measurement of the states connecting the $E2$ transitions to the yrast levels.

V. CONCLUSIONS

The precessions of statistical γ rays, of the $E2$ “bump” high-energy radiations with $1200 < E_\gamma < 2000$ keV and of the yrast discrete γ rays, have been determined in a transient field measurement, resulting in information on the time evolution of the decay in the region of $31\hbar < I < 56\hbar$. The data from this experiment are consistent with the results of a Monte Carlo simulation which simultaneously reproduces the experimentally measured Doppler shifts, multiplicities, and spectral shapes with a unique set of parameters, $\langle J \rangle_{\text{eff}}$, $\langle Q \rangle_t$ [6].

The average g factor of the ensemble of all states probed is small: $\langle g \rangle = 0.21(2)$. If it is assumed that the $E2$ collective states have an average g factor of $g = Z/A$, the average g factor of the states just above the yrast line at $31\hbar < I < 35\hbar$ can be separately determined: $\langle g \rangle = 0.14(2)$. These data point to a significant contribution from aligned neutrons to the total spin of these states. A similar result of a reduced g factor, and the corresponding implication of neutron alignment, was found in high-spin regions in other rare-earth nuclei such as ¹⁵⁶Dy [3] and ^{158,160,162}Yb [5].

In summary, the data from this experiment support the model that has been developed in Refs. [6] and [15] for the decay of excited quasicontinuum states. The measured precessions also confirm the short emission times of the $E2$ transitions and, hence, the collective character of the excited states deduced in the earlier experiments. In order to obtain a sharper picture of the evolution of the decaying structure, additional experiments, with a thinner gadolinium foil (which would probe only the $E2$ component) or with a buffer layer between the target and gadolinium (which would exclude the $E2$ component), are being prepared.

ACKNOWLEDGMENTS

We would like to thank Dr. Peter Maier-Komor for the preparation of the gadolinium foils and Dr. R. Tanczyn for measuring their magnetization. The authors also express their gratitude to J. Goral, J. Timm, and J. Joswich for technical assistance with the cooling of the gadolinium foils and to P. Wilt for his help with the electronics of the rotating magnet assembly. This work was supported by the U.S. Department of Energy, Nuclear Physics Division, under Contracts No. W-31-109-ENG-38 (for ANL) and No. DE-FG02-87ER40A0346 (for Purdue) and supported in part by the NSF (for Rutgers, Rochester, and Notre Dame).

*On leave from the Weizmann Institute of Science, Rehovot, Israel.

†Present address: University of Rochester, NSRL, Rochester, NY 14627.

[1] G. Seiler-Clark, D. Pelte, H. Emling, A. Balanda, H. Grein, E. Grosse, R. Kulesa, D. Schwalm, H. J. Wollersheim, M. Hass, G. J. Kumbartzki, and K.-H. Speidel, Nucl. Phys. A399, 211 (1983).

[2] O. Häusser, H. Graf, L. Grodzins, E. Jaeschke, V. Metag, D. Habs, D. Pelte, H. Emling, E. Grosse, R. Kulesa, D. Schwalm, R. S. Simon, and J. Keikonen, Phys. Rev. Lett. 48, 383 (1982).

[3] N. Rud, D. Ward, H. R. Andrews, O. Häusser, P. Taras, J. Keikonen, M. Neiman, R. M. Diamond, and F. S. Stephens, Phys. Lett. 101B, 35 (1981); O. Häusser, D. Ward, H. R. Andrews, P. Taras, B. Haas, M. A.

- Deleplanque, R. M. Diamond, E. L. Dines, A. O. Macchiavelli, and C. V. Stager, *ibid.* **144B**, 341 (1984).
- [4] W. Reviol, Ph.D. thesis, Freie Universität Berlin, 1988.
- [5] E. Lubkiewicz, H. Emling, H. Grein, R. Kulesa, R. S. Simon, H. J. Wollersheim, Ch. Ender, J. Gerl, D. Habs, and D. Schwalm, *Z. Phys. A* **335**, 369 (1990).
- [6] R. Holzmann, I. Ahmad, B. K. Dichter, H. Emling, R. V. F. Janssens, T. L. Khoo, W. C. Ma, M. W. Drigert, U. Garg, D. C. Radford, P. J. Daly, Z. Grabowski, H. Helpi, M. Quader, and W. Trzaska, *Phys. Lett. B* **195**, 321 (1987).
- [7] N. Benczer-Koller, M. Hass, and J. Sak, *Annu. Rev. Nucl. Sci.* **30**, 53 (1980).
- [8] M. Hass, I. Ahmad, R. V. F. Janssens, T. L. Khoo, H. J. Korner, E. F. Moore, F. H. L. Wolfs, N. Benczer-Koller, E. Dafni, K. Beard, U. Garg, P. J. Daly, and M. Piiparinen, *Phys. Rev. C* **39**, 2237 (1989).
- [9] The velocity profile in the target assembly was calculated with the stopping powers presented by J. F. Ziegler, J. P. Biersack, and U. Littmark, in *The Stopping and Range of Ions in Solids*, Vol. 1 of *The Stopping and Range of Ions in Matter*, edited by J. F. Ziegler (Pergamon, New York, 1985).
- [10] B. M. Nyakó, J. Simpson, P. J. Twin, D. Howe, P. D. Forsyth, and J. F. Sharpey-Schafer, *Phys. Rev. Lett.* **56**, 2680 (1986).
- [11] M. A. Bentley, A. Alderson, G. C. Ball, H. W. Cranmer-Gordon, P. Fallon, B. Fant, B. Herskind, D. Howe, C. A. Kalfas, A. R. Mokhtar, J. D. Morrison, A. H. Nelson, B. M. Nyakó, K. Schiffer, J. F. Sharpey-Schafer, J. Simpson, G. Sletten, and P. J. Twin, *J. Phys. G* **17**, 481 (1991).
- [12] D. C. Radford, I. Ahmad, R. Holzmann, R. V. F. Janssens, and T. L. Khoo, *Nucl. Instrum. Methods A* **258**, 111 (1987).
- [13] O. Häusser, H. R. Andrews, D. Horn, M. A. Lone, P. Taras, P. Skensved, R. M. Diamond, M. A. Deleplanque, E. L. Dines, A. Macchiavelli, and F. S. Stephens, *Nucl. Phys. A* **412**, 141 (1984).
- [14] J. F. Ziegler, in *Handbook of Stopping Cross Sections for Energetic Ions in all Elements*, Vol. 5 of *The Stopping and Ranges of Ions in Matter*, edited by J. F. Ziegler (Pergamon, New York, 1980); H. H. Anderson and J. F. Ziegler, in *Hydrogen Stopping Powers and Ranges in all Elements*, Vol. 3 of *The Stopping and Ranges of Ions in Matter*, edited by J. F. Ziegler (Pergamon, New York, 1977).
- [15] R. Holzmann, T. L. Khoo, W. C. Ma, I. Ahmad, B. K. Dichter, H. Emling, R. V. F. Janssens, M. W. Drigert, U. Garg, M. A. Quader, P. J. Daly, M. Piiparinen, and W. Trzaska, *Phys. Rev. Lett.* **62**, 520 (1989).
- [16] A. Bohr and B. R. Mottelson, *Nuclear Structure* (Benjamin, New York, 1969), Vol. 1.
- [17] G. A. Bartholomew, E. D. Earle, A. J. Ferguson, J. W. Knowles, and M. A. Lone, in *Advances in Nuclear Physics*, edited by J. W. Negele and E. Voigt (Plenum, New York, 1973), Vol. 7.
- [18] B. Lauritzen, T. Dössing, and R. Broglia, *Nucl. Phys. A* **457**, 61 (1986).
- [19] G. Leander, *Phys. Rev. C* **25**, 2780 (1982).